Translational Stroke Research (2019) 10:695–704
https://doi.org/10.1007/s12975-019-0687-6

ORIGINAL ARTICLE

Dynamic Detection of Thrombolysis in Embolic Stroke Rats by Synchrotron Radiation Angiography

Liping Wang[1] · Panting Zhou[2] · Zhihao Mu[3] · Xiaojie Lin[2] · Lu Jiang[2] · Zhuo Cheng[2,4] · Longlong Luo[2] · Zhiming Xu[5] · Jieli Geng[6] · Yongting Wang[2] · Zhijun Zhang[2] · Guo-Yuan Yang[1,2]

Received: 3 August 2018 / Revised: 30 November 2018 / Accepted: 3 January 2019 / Published online: 24 January 2019

Abstract

A rodent model of embolic middle cerebral artery occlusion is used to mimic cerebral embolism in clinical patients. Thrombolytic therapy is the effective treatment for this ischemic injury. However, it is difficult to detect thrombolysis dynamically in living animals. Synchrotron radiation angiography may provide a novel approach to directly monitor the thrombolytic process and assess collateral circulation after embolic stroke. Thirty-six adult Sprague-Dawley rats underwent the embolic stroke model procedure and were then treated with tissue plasminogen activator. The angiographic images were obtained in vivo by synchrotron radiation angiography. Synchrotron radiation angiography confirmed the successful establishment of occlusion and detected the thrombolysis process after the thrombolytic treatment. The time of thrombolytic recanalization was unstable during embolic stroke. The infarct volume increased as the recanalization time was delayed from 2 to 6 h ($p < 0.05$). The collateral circulation of the internal carotid artery to the ophthalmic artery, the olfactory artery to the ophthalmic artery, and the posterior cerebral artery to the middle cerebral artery opened after embolic stroke and manifested different opening rates (59%, 24%, and 75%, respectively) in the rats. The opening of the collateral circulation from the posterior cerebral artery to the middle cerebral artery alleviated infarction in rats with successful thrombolysis ($p < 0.05$). The cerebral vessels of the circle of Willis narrowed after thrombolysis ($p < 0.05$). Synchrotron radiation angiography provided a unique tool to dynamically detect and assess the thrombolysis process and the collateral circulation during thrombolytic therapy.

Keywords Angiography · Collateral circulation · Ischemia · Thrombolysis · Synchrotron radiation

Liping Wang and Panting Zhou contributed equally to this work.

✉ Zhijun Zhang
zhangzj@sjtu.edu.cn

✉ Guo-Yuan Yang
gyyang@sjtu.edu.cn

[1] Department of Neurology, Ruijin Hospital, School of Medicine, Shanghai Jiao Tong University, Shanghai 200025, China

[2] Med-X Research Institute and School of Biomedical Engineering, Shanghai Jiao Tong University, 1954 Hua Shan Road, Shanghai 200030, China

[3] Department of Pathology and Pathophysiology, Faculty of Basic Medical Sciences, Kunming Medical University, Kunming 650500, China

[4] Chongqing Health Information Center, Chongqing 400000, China

[5] Department of Neurosurgery, Shanghai Jiao Tong University Affiliated Sixth People's Hospital, Shanghai 200030, China

[6] Department of Neurology, Shanghai Renji Hospital, School of Medicine, Shanghai Jiao Tong University, Shanghai 200025, China

Abbreviations

ACA	Anterior cerebral artery
DSA	Digital subtraction angiography
ECA	External carotid artery
eMCAO	Embolic middle cerebral artery occlusion
ICA	Internal carotid artery
ID	Internal diameter
MCA	Middle cerebral artery
MRI	Magnetic resonance imaging
PCA	Posterior cerebral artery
SD rats	Sprague–Dawley rats
SR	Synchrotron radiation
tPA	Tissue plasminogen activator

Introduction

Cerebral ischemia is a major cause of mortality and disability worldwide [1–3]. Approximately 40% of ischemic strokes are

caused by proximal intracranial large vessel occlusion [4]. Until now, thrombolytic therapy and endovascular thrombectomy have been the only effective treatments for ischemic stroke in the acute phase [5, 6]. Thrombolytic therapy with tissue plasminogen activator (tPA) is beneficial when given within 4.5 h of ischemic onset [7, 8]. However, hemorrhagic transformation, neurotoxicity, and treatment within a narrow window of time comprise major limitations for thrombolytic therapy, resulting in only a few patients benefiting from it [9]. Therefore, dynamically detecting vascular changes following thrombolytic therapy should be further studied. The experimental animal model plays a critical role in basic research. Embolic middle cerebral artery occlusion (eMCAO) model in rodents is used to mimic cerebral embolism in clinical patients. Stability is the key property of the animal model, which can seriously affect the experimental results. In addition, monitoring the course of thrombolysis in real-time is important for the assessment of results.

The collateral circulation of the brain refers to the existing or neo-formed vascular bypass in the brain. When cerebral vascular diseases induce the reduction of blood supply, the blood flow can reach the ischemic zone through collateral circulation. The ischemic zone is compensated with different degrees of perfusion. Collateral circulation is the key element setting the pace of the ischemic process. The collateral score could be an independent predictor of final infarct volume and improvement in the clinical deficit [10, 11]. After arterial occlusion, collateral blood flow modulates the temporal growth of the ischemic core into the penumbral area [4]. Conventional imaging technology restricts the basic research of collateral circulation in vivo. At present, the study of collateral circulation has had a minor advancement. Collateral circulation assessment is used more as a predictor of the outcome after treatment, and it has not yet reached the extent of affecting the clinical decision. Therefore, the collateral circulation assessment should be further optimized, and the degree of collateral circulation needs to be quantified to provide more reliable information for clinical therapy.

Common devices applied to the visual study of cerebral vasculature in living animals included optical imaging, CT angiography, digital subtraction angiography (DSA), MR angiography (MRA), and color Doppler ultrasonography [12–15]. However, the low resolution of these methods limits the detection of microvasculature disorders [16, 17]. Synchrotron radiation (SR) X-ray imaging could reach the submicron range of spatial resolution. The resolution of SR is approximately 1000 times higher than that of conventional X-ray absorption imaging [18, 19]. Recently developed SR angiography has provided a unique tool to monitor real-time hemodynamic changes in blood flow and microvascular morphology [20–22]. Based on this, we attempted to perform SR angiography in order to explore collateral circulation after eMCAO, the process of thrombolysis, and vascular changes after thrombolysis.

In this study, we aim to (1) establish a novel method of dynamic thrombolysis detection, (2) evaluate the collateral circulation after eMCAO, and (3) explore the effect of tPA thrombolytic therapy on vascular diameter and perfusion.

Materials and Methods

Animals and Experimental Groups

Animal procedures were reviewed and approved by the Institutional Animal Care and Use Committee (IACUC) of Shanghai Jiao Tong University, Shanghai, China. Adult male Sprague-Dawley (SD) rats ($n = 36$) weighing 250 ± 30 g (Sippr-BK, Inc., Shanghai, China) were used in the study. Animal studies were reported according to ARRIVE guidelines. The animals were housed normally with free access to water and food. After ischemic stroke, the animals were administered an intravenous dose of 10 mg/kg of tPA (Boehringer Ingelheim, Ingelheim, Germany) as the thrombolytic therapy, which was administered 3 h after eMCAO [7, 8, 23].

Embolic MCAO Models

A homologous clot was prepared 1 day before the eMCAO surgery. A blood donor rat was anesthetized by isoflurane (RWD, Shenzhen, China). A 250-mm PE-50 tube was inserted into the femoral artery, and fresh arterial blood was withdrawn using a 2.5-ml syringe and into the tube to form the homologous clot. The clot was maintained in the tube at room temperature for 2 h and was subsequently stored at 4 °C for 22 h. Then, the PE-50 tube containing the clot was cut to the length of 40 mm. The clot was transferred into a dish containing saline and then inhaled into the PE-04-50 tube with a 2.5-ml syringe before use.

Rats were anesthetized by isoflurane, and an incision was made in the middle of the neck of the rat to expose the common carotid artery (CCA), internal carotid artery (ICA), and external carotid artery (ECA) under the microscope. The PE-04 catheter containing a single fibrin-rich clot was introduced into the ECA lumen through the small incision. The tip of the catheter was approximately 2 to 3 mm from the origin of the middle cerebral artery (MCA). The clot was gently injected into the ICA. After 5 min, the catheter was withdrawn [24–26].

SR Angiography in Living Animals

SR angiography was conducted at the X-ray imaging beam line BL13W in Shanghai Synchrotron Radiation Facility.

Imaging procedures have been described previously [27]. The average beam current was 145 mA, and X-ray energy was 33.2 keV. Rats were anesthetized intraperitoneally with ketamine/xylazine (100 mg/10 mg/kg) during the imaging process. An angiographic tube was inversely inserted into the ECA to inject 160 μl of diluted iodinated contrast medium, Ipamiro (General Electric Company, Shanghai, China), into the CCA at a rate of 6 ml/min using an automated microsyringe pump (LSP01-1A, Longer; Baoding, China). An X-ray complementary metal oxide semiconductor (pixel size 9.0 μm × 9.0 μm, frame frequency 30 Hz, Hamamatsu Ltd., Japan) was utilized to record high-resolution real-time angiographic images. Next, MATLAB software (MathWorks, Natick, MA) with a written short program was used to identify perfused vessels from the original SR angiography images [28].

MRI

Magnetic resonance imaging (MRI) was performed on animals 1 day after eMCAO. MRI experiments were performed on a 3T General Electric MR system (GE Medical Systems, South San Francisco, CA). Rats were intraperitoneally anesthetized with ketamine/xylazine (100 mg/10 mg/kg, Fujian Gutian Pharmaceutical Co., Ltd., Gutian, China/Sigma-Aldrich, St. Louis, MO). The heads of the rats were placed approximately at the center of a homemade coil. The rats were secured in a prone position. All brains were examined by T2-weighted MRI with imaging parameters: TR = 2000 ms, TE = 40 ms, matrix = 160 × 192, FOV = 60.0 × 60.0 mm, slice thickness = 1.0 mm, and interslice distance = 0 mm [29].

TTC Staining

2,3,5-Triphenyltetrazolium chloride (TTC) staining was performed to detect the infarct area. One day after eMCAO, animal brains were removed immediately and coronal slices were dissected using a brain slicer. The brain slices were stained with 2% TTC in Dulbecco's phosphate buffer (pH 7.4) at 37 °C for 20 min [30]. The ischemic lesion area could not be colored red. Infarct volume was calculated by ImageJ software (National Institutes of Health, Bethesda, MD) as described previously [31].

HE Staining

Rats were sacrificed 1 day after eMCAO and perfused with saline followed by 4% paraformaldehyde transcardially. After fixation and dehydration, the brains were embedded in paraffin and made into a series of 8-μm-thick coronal sections. Then, we performed hematoxylin and eosin (HE) staining according to our previously reported procedures [27, 32]. Sections were immersed into hematoxylin dye for 5 min. Next, brain sections were immersed into eosin dye for 30 s followed by dehydration with 95% ethanol and clarity with dimethylbenzene.

Hemorrhagic Transformation Identification

Rats were sacrificed after eMCAO and perfused transcardially with saline followed by 4% paraformaldehyde. If hemorrhagic transformation occurred, blood was observed in the brain tissue instead of the vessels. Otherwise, the brain color was light yellow except for the embolus.

Dimeter Assessment of Cerebral Vessels

Measurements of the vessel internal diameters (ID) of the extracranial ICA, intracranial ICA, MCA, posterior cerebral artery (PCA), and anterior cerebral artery (ACA) were conducted using image analysis ImageJ software (National Institutes of Health). The vessel ID represents the average of three independent measurements [28]. The investigator who performed the measurements was unaware whether the angiographic images were captured before eMCAO or after tPA thrombolysis.

Statistical Analysis

Data were presented as the mean ± SD. The infarct volumes for multiple comparisons among different recanalization time groups were evaluated using one-way ANOVA followed by Tukey's post hoc test. The infarct volume affected by collateral circulation and the comparisons of repeated diameter measurements were assessed by one-way ANOVA followed by the Bonferroni test. Data were assessed using SPSS software (SPSS Inc., Armonk, NY). A probability value of less than 5% was considered to represent statistical significance.

Results

The Establishment of eMCAO

The SR angiographic images detected the entire vasculature of the left hemisphere including ICA, MCA, ACA, PCA, small arteries, and small veins. The images showed that the MCA was occluded after eMCAO (Fig. 1a). The MRI demonstrated the lesion area after eMCAO (Fig. 1b). The stereo-microscopic images of rat brain indicated the location of the emboli (Fig. 1c). HE staining was performed to detect that the injected emboli obstructed the lumen (Fig. 1d). We found emboli blocking the arteries. The white area in the TTC staining represented the lesion area (Fig. 1e). The mortality rate was 8.33%. The success rate of the eMCAO model was 77.8%.

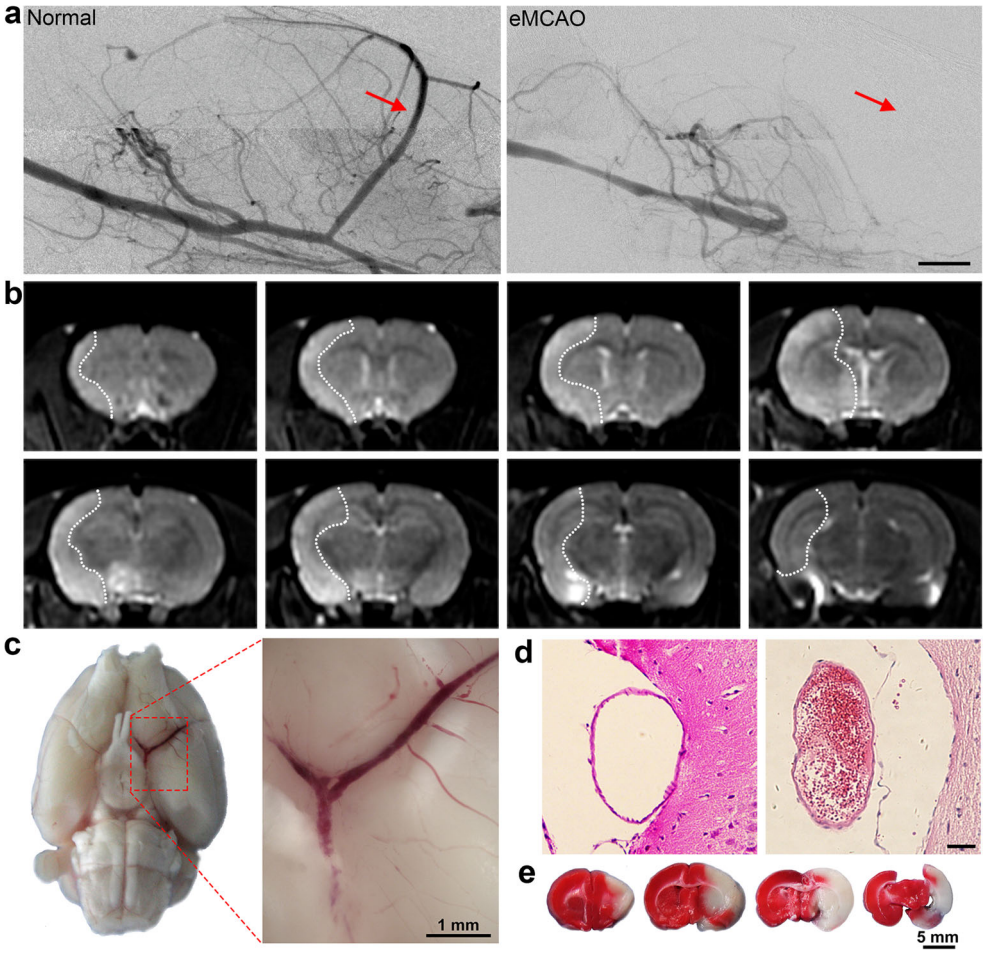

Fig. 1 The establishment of eMCAO. **a** SR angiographic images of the normal rat and the rat after eMCAO. The red arrow indicated the location of MCA. The MCA was occluded after eMCAO. Bar = 1 mm. **b** MRI of the rat after eMCAO. The white dotted line demonstrated the lesion area. **c** Stereo-microscopic images of the rat brain after eMCAO. **d** HE staining showed the lumen without emboli and the lumen with emboli. Bar = 50 μm. **e** Coronal sections of rat brain, from anterior to posterior. The white area in the TTC staining represented the lesion area

The Dynamic Detection of Thrombolysis

The synchrotron radiation angiographic images showed that there was no blood flow in the MCA and ACA after eMCAO. After tPA injection, successful thrombolysis could be observed by SR angiography. However, there were some failed cases of thrombolysis (Fig. 2a). The failed thrombolysis rate was 21.4%. The stereo-microscopic images of rat brain demonstrated the red embolus located in the circle of Willis in rats with failed thrombolysis, while there were no emboli in rats with successful thrombolysis (Fig. 2b). Rats with failed thrombolysis did not present with hemorrhage. Hemorrhagic transformation arose in some of the rats with successful thrombolysis (Fig. 2c). The hemorrhagic transformation rate was 10.7%.

The Time of Thrombolytic Recanalization Was Not Stable in eMCAO

The dynamic angiographic data indicated that the thrombolytic recanalization time was not stable. Our observation time lasted 12 h. We observed that most of the thrombolysis cases occurred within 6 h after tPA administration. However, in some of the failed cases, the MCA did not re-perfuse during our observation time (Fig. 3a–d). Nearly 50% of thrombolysis occurred between 1 and 6 h after tPA administration (Fig. 3e). There were no differences in the infarct volume among the groups with recanalization within 2 h. The infarct volumes were higher in the 2.0–6.0 h group and failed recanalization group compared to the 0.0–0.5 h group (Fig. 3f, $p < 0.05$). The infarct volume increased as the recanalization time was delayed from 2 to 6 h (Fig. 3f, $p < 0.05$).

Collateral Circulation Opened After eMCAO in Rats

Hemisphere microvasculature in rats was dynamically revealed by SR angiography after eMCAO to explore the collateral circulation (Fig. 4a). We directly observed the collateral circulations from the ICA to the ophthalmic artery (OphA), the olfactory artery (OA) to the OphA, and the PCA to the MCA (Fig. 4b). Data analysis showed that the open ratios of ICA-OphA, OA-OphA, and PCA-MCA after eMCAO were 58.82%, 23.53%, and 75.00%, respectively (Fig. 4c). The collateral circulation PCA-MCA opening alleviated the infarction in rats with successful thrombolysis (Fig. 4d, $p < 0.05$).

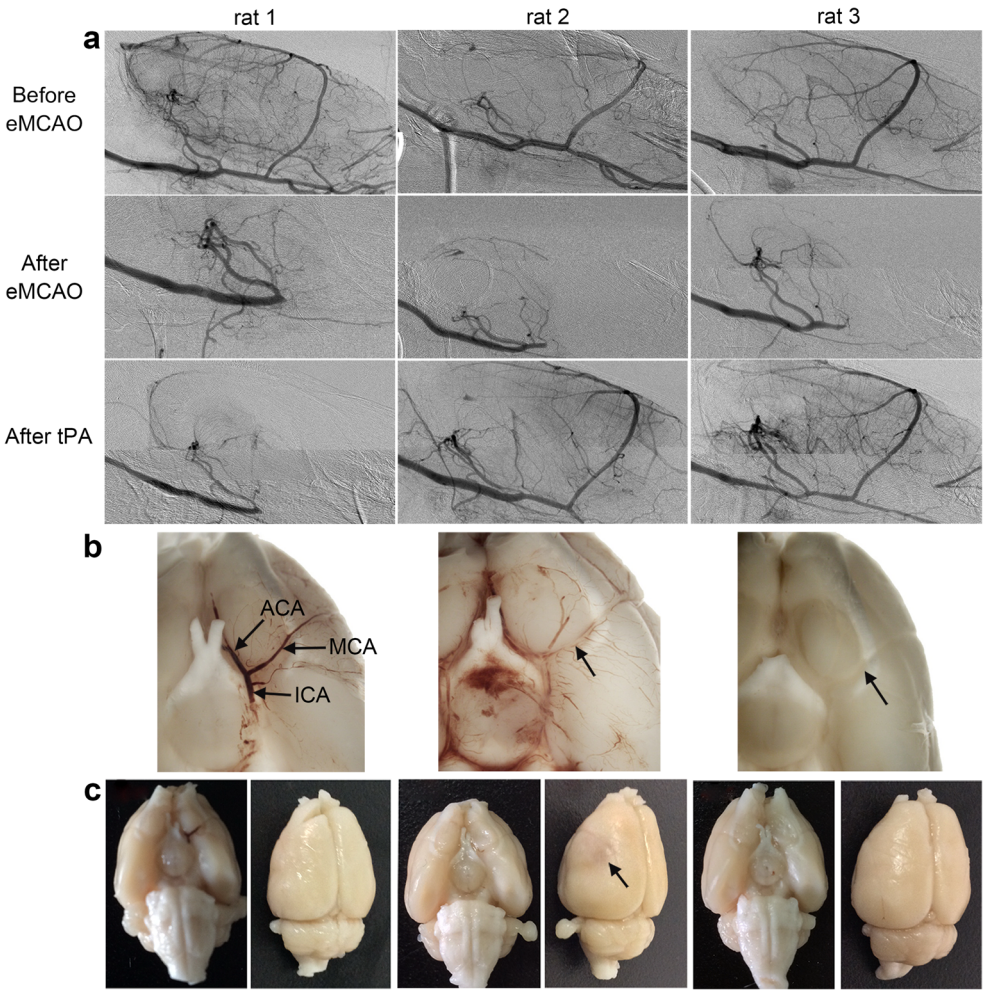

Fig. 2 The dynamic detection of thrombolysis. **a** SR angiographic images of the rat before eMCAO, after eMCAO and after tPA. Thrombolysis was successful in rats 2 and 3 while failed in rat 1. **b** Stereo-microscopic images of the rat brain. The red embolus was located in the circle of Willis in rat 1, while there were no emboli in rats 2 or 3. **c** Images showed that the hemorrhage in rat 2 after thrombolysis

The Cerebral Vessels of the Circle of Willis Narrowed After tPA Thrombolysis

The diameters of extracranial ICA, intracranial ICA, PCA, MCA, and ACA according to the angiographic images before eMCAO and after thrombolysis were measured by an investigator who was blind to the experimental groups. The data showed that the diameter of extracranial ICA, intracranial ICA, MCA, and ACA became narrow at the time-point of recanalization, which indicated decreased blood flow (Fig. 5, $p < 0.05$).

Discussion

The eMCAO model is commonly used in focal cerebral ischemic research. At this time, thrombolytic therapy demonstrates to improve outcomes from acute ischemic stroke. We established a novel method to dynamically monitor the process of thrombolysis with tPA following eMCAO. The risk of intracerebral hemorrhage and the narrow time window limited the use of tPA for stroke [23]. Extending the narrow time window of tPA could benefit a significant number of stroke patients [7]. This situation calls for the further development of thrombolytic drugs. SR angiography could be used in animal research yielding higher resolution than DSA, which is commonly used in the clinic. This technique could be beneficial to the basic study of thrombolysis.

Our results suggested that the recanalization time with tPA after eMCAO was unstable. The recanalization time varied greatly after tPA administration, which affected the infarct. The variability in cerebrovascular anatomy between the individual rats might affect the results. The factors causing variation should be further explored. In addition, we detected that few rats underwent hemorrhagic transformation after tPA treatment. The hemorrhagic transformation was likely due to the effect of tPA on the breakdown of the blood-brain barrier [7].

It was interesting that we found that the vascular diameter of the circle of Willis decreased after successful thrombolysis with tPA. This phenomenon suggested that the blood perfusion after thrombolysis was lower than that under normal physiological conditions and might be caused by the post-recanalization vasospasm in the circle of Willis. Post

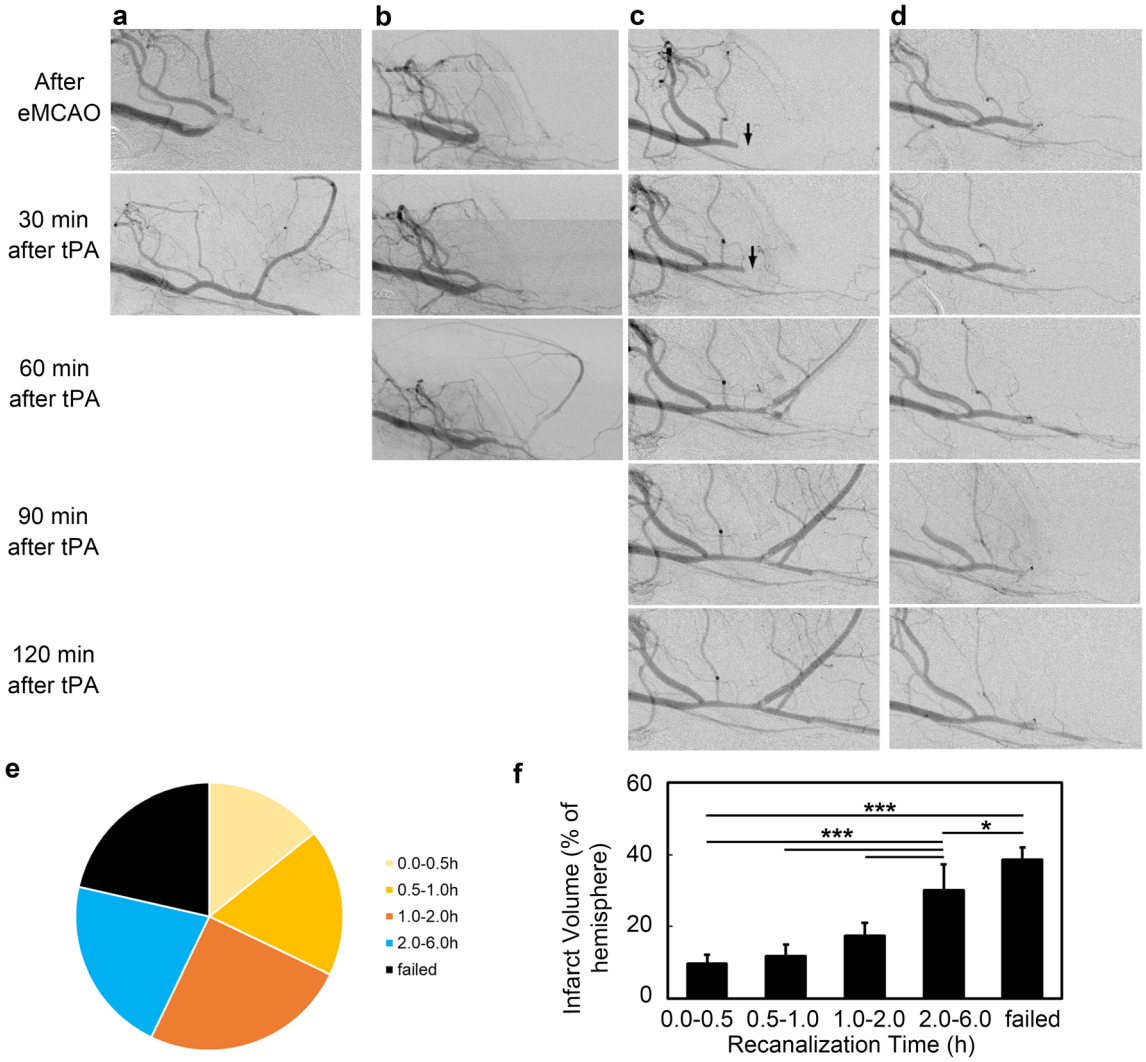

Fig. 3 The time of thrombolytic recanalization was not stable in eMCAO. Dynamic angiographic images of the rat after eMCAO, 30 min after tPA, 60 min after tPA, 90 min after tPA, and 120 min after tPA. **a** Thrombolytic recanalization occurred 30 min after tPA application. **b** Thrombolytic recanalization occurred 60 min after tPA application. **c** Thrombolytic recanalization occurred 120 min after tPA application, but there was still a small embolus in the MCA. Arrows indicated the residual embolus. **d** The tPA thrombolysis failed. The MCA was not reperfused. **e** Pie graph showing the incidence of the different recanalization times. **f** Bar graph showed the relationship between the recanalization time and infarction. Data are shown as the mean ± SD, $n = 4–7$ per group. $^{*}p < 0.05$; $^{**}p < 0.01$; $^{***}p < 0.001$

reperfusion vasospasm and no-reflow have been reported previously. No-reflow after reperfusion in the brain might involve cortical spreading depression with disturbed local vascular control, high level of extracellular K^+, endothelial cell swelling, pericyte contraction, interstitial edema, and inflammation [33, 34].

Our data demonstrated that SR angiography could detect collateral circulation after eMCAO in vivo. Collateral circulation includes three levels. The circle of Willis is the first level of collateral circulation. The ophthalmic anastomoses from the pterygopalatine artery and leptomeningeal anastomoses from the ACA constitute the secondary level. The angiogenesis and arteriogenesis in the brain increasing the local blood flow comprise the third level [35–37]. Recent studies have found that clinical DWI mismatch, defined as National Institutes of Health Stroke Scale score ≥ 8 and DWI ischemic volume ≤ 25 mL, suggested to have fine collateral circulation [38]. Therefore, collateral circulation is vital for the development of ischemic stroke. DSA is the gold standard for assessing collateral circulation [39]. Our image processing technique resembles DSA, but SR angiography has a higher resolution, providing a clear view of the vasculature, especially in experimental small animal models. The common factors that affect the opening of collateral circulation include dehydration in high temperature, hyperglycemia, increase in blood viscosity, electrolyte disturbance, heart failure, renal insufficiency, decrease in blood pressure, atherosclerosis, and hypertension. These risk factors are worth noting to promote the

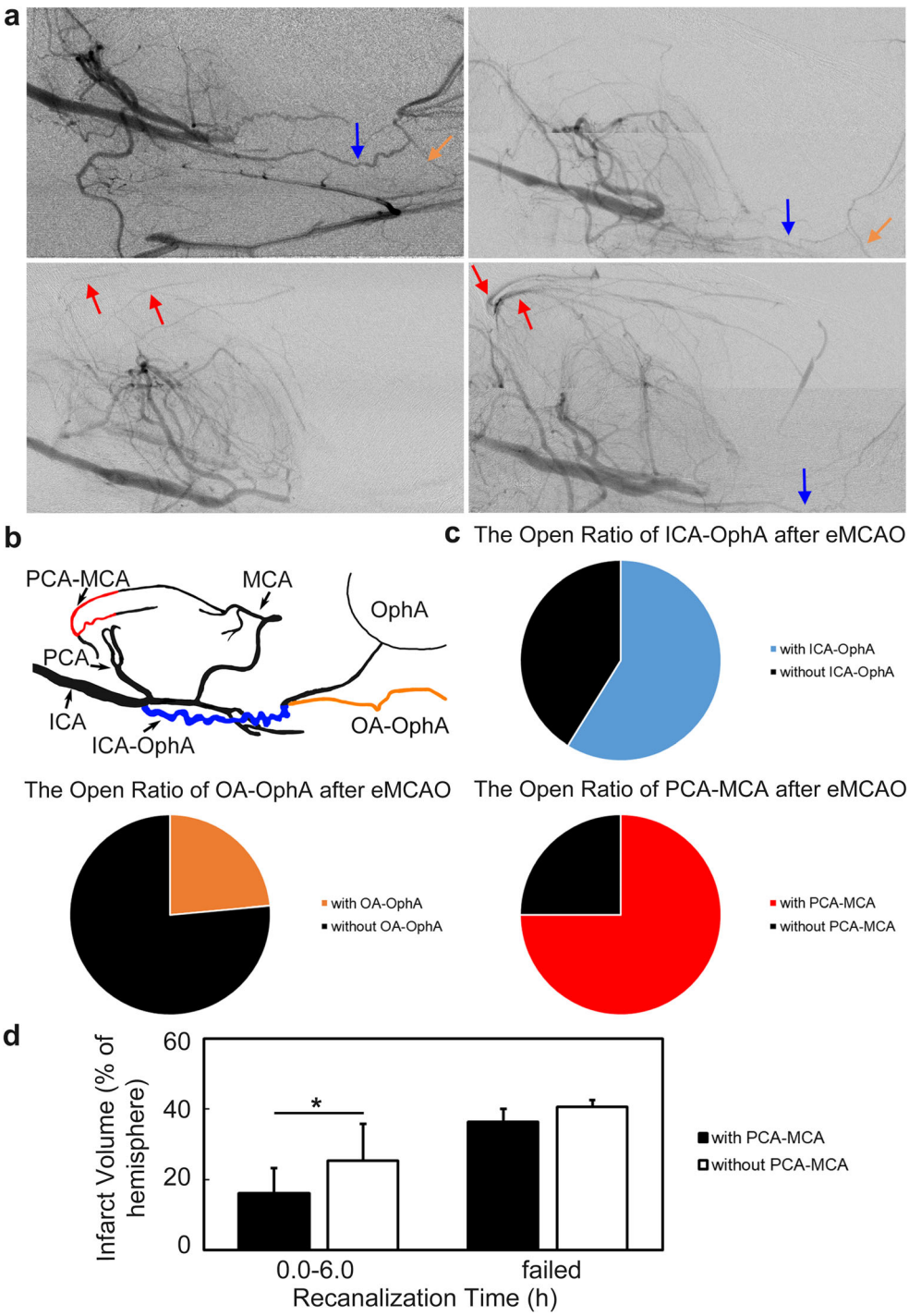

Fig. 4 The SR angiographic images of collateral circulation after eMCAO in rats. **a** Angiographic images of rat brain vascular morphology after eMCAO. Blue, orange, and red arrows indicated collateral circulation from the ICA to OphA, the OA to OphA, and the PCA to MCA, respectively. **b** Schematic diagram of collateral circulation from the ICA to OphA, the OA to OphA and the PCA to MCA. **c** Pie charts showing the open ratio of ICA-OphA, OA-OphA, and PCA-MCA after eMCAO. **d** Bar graph showed the relationship between the opening of PCA-MCA and the infarct volume. Data are shown as the mean ± SD, $n = 3$–18 per group. $^*p < 0.05$

opening rate of collateral circulation when stenosis or occlusion occurs in the ICA. Although the collateral circulation assessment needs to be improved, the development of imaging techniques is relatively slow. Moreover, the importance of collateral circulation after ischemic stroke in basic research does not receive much consideration. SR angiography could contribute to the optimization of collateral circulation assessment and guide clinical practice. This method also sheds light on the investigation of promoting the opening of collateral circulation to rescue the ischemic zone.

There are some limitations in our study. Although SR angiography is beneficial to the basic study of thrombolysis, collateral circulation, and experimental model modification, it is difficult to apply to the broader community. We did not apply SR angiography in other strains of rats. Thus, we cannot be sure of whether the results could be affected by the rat strain. In addition, potential differences between males and

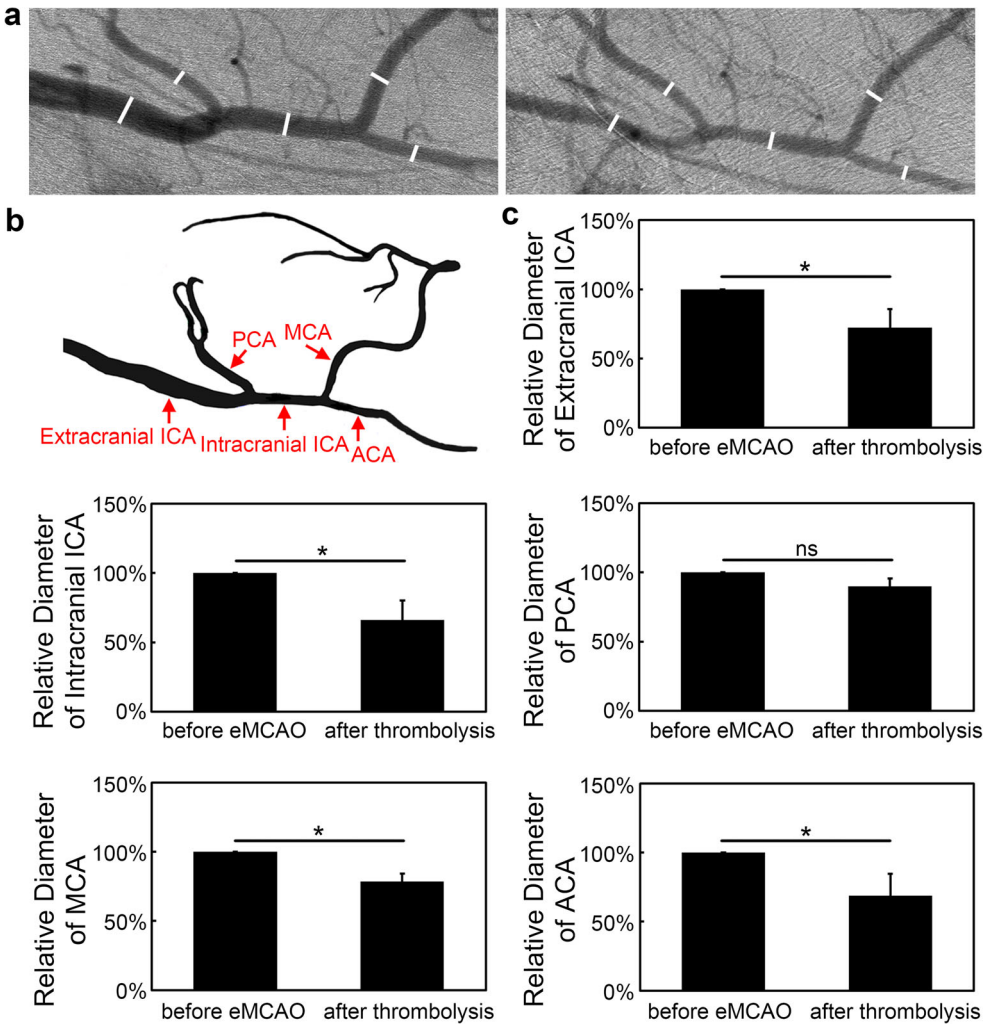

Fig. 5 The cerebral vessels of the circle of Willis narrowed after tPA thrombolysis. **a** SR angiographic images of a rat before eMCAO and after thrombolysis. **b** The schematic diagram showed where the diameters of the extracranial ICA, intracranial ICA, PCA, MCA, and ACA were measured. **c** Bar graphs showed the relative diameter of the extracranial ICA, intracranial ICA, PCA, MCA, and ACA before eMCAO and after thrombolysis. Data are shown as the mean ± SD. $n = 3$ per group; $^*p < 0.05$

females in regard to the time variability in thrombolysis and in the opening of collateral circulation still need to be explored.

In summary, we performed SR angiography to dynamically study the thrombolysis process after tPA treatment in eMCAO rats. The infarct volume increased as the recanalization time was delayed from 2 to 6 h. The rats manifested different opening rates of collateral circulation including ICA to OphA, OA to OphA, and PCA to MCA after eMCAO. The collateral circulation of the PCA to MCA opening alleviated the infarct after eMCAO. Additionally, the cerebral vessels of the circle of Willis narrowed after tPA thrombolysis, which might affect blood perfusion. SR angiography provided a unique tool to dynamically detect and assess the thrombolysis process and collateral circulation during thrombolytic therapy.

Acknowledgements The authors thank BL13W station at Shanghai Synchrotron Radiation Facility.

Funding This study was supported by grants from the National Natural Science Foundation of China (81771251, GYY; 81771244, ZJZ), the National Key Research and Development Program of China (2016YFC1300600), K. C. Wong Education Foundation (GYY), and the Science and Technology Commission of Shanghai Municipality (17ZR1413600, ZJZ).

Compliance with Ethical Standards

Conflict of Interest The authors declare that they have no conflict of interest.

Ethical Approval All applicable international, national, and/or institutional guidelines for the care and use of animals were followed.

Informed Consent Informed consent was obtained from all individual participants included in the study.

Publisher's Note Springer Nature remains neutral with regard to jurisdictional claims in published maps and institutional affiliations.

References

1. Strong K, Mathers C, Bonita R. Preventing stroke: saving lives around the world. Lancet Neurol. 2007;6(2):182–7. https://doi.org/10.1016/S1474-4422(07)70031-5.

2. George PM, Steinberg GK. Novel stroke therapeutics: unraveling stroke pathophysiology and its impact on clinical treatments. Neuron. 2015;87(2):297–309. https://doi.org/10.1016/j.neuron.2015.05.041.
3. Krishnamurthi RV, Feigin VL, Forouzanfar MH, Mensah GA, Connor M, Bennett DA, et al. Global and regional burden of first-ever ischaemic and haemorrhagic stroke during 1990-2010: findings from the global burden of disease study 2010. Lancet Glob Health. 2013;1(5):e259–81. https://doi.org/10.1016/S2214-109X(13)70089-5.
4. Rocha M, Jovin TG. Fast versus slow progressors of infarct growth in large vessel occlusion stroke: clinical and research implications. Stroke. 2017;48(9):2621–7. https://doi.org/10.1161/STROKEAHA.117.017673.
5. Goyal M, Menon BK, van Zwam WH, Dippel DW, Mitchell PJ, Demchuk AM, et al. Endovascular thrombectomy after large-vessel ischaemic stroke: a meta-analysis of individual patient data from five randomised trials. Lancet. 2016;387(10029):1723–31. https://doi.org/10.1016/S0140-6736(16)00163-X.
6. Lyden P, Lu M, Kwiatkowski T, Frankel M, Levine S, Broderick J, et al. Thrombolysis in patients with transient neurologic deficits. Neurology. 2001;57(11):2125–8.
7. dela Pena IC, Yoo A, Tajiri N, Acosta SA, Ji X, Kaneko Y, et al. Granulocyte colony-stimulating factor attenuates delayed tPA-induced hemorrhagic transformation in ischemic stroke rats by enhancing angiogenesis and vasculogenesis. J Cereb Blood Flow Metab. 2015;35(2):338–46. https://doi.org/10.1038/jcbfm.2014.208.
8. Ishiguro M, Mishiro K, Fujiwara Y, Chen H, Izuta H, Tsuruma K, et al. Phosphodiesterase-III inhibitor prevents hemorrhagic transformation induced by focal cerebral ischemia in mice treated with tPA. PLoS One. 2010;5(12):e15178. https://doi.org/10.1371/journal.pone.0015178.
9. Ishiguro M, Kawasaki K, Suzuki Y, Ishizuka F, Mishiro K, Egashira Y, et al. A rho kinase (ROCK) inhibitor, fasudil, prevents matrix metalloproteinase-9-related hemorrhagic transformation in mice treated with tissue plasminogen activator. Neuroscience. 2012;220:302–12. https://doi.org/10.1016/j.neuroscience.2012.06.015.
10. Agarwal S, Bivard A, Warburton E, Parsons M, Levi C. Collateral response modulates the time-penumbra relationship in proximal arterial occlusions. Neurology. 2017;90:e316–22. https://doi.org/10.1212/WNL.0000000000004858.
11. Jiang W, Hu W, Ye L, Tian Y, Zhao R, Du J et al. Contribution of Apelin-17 to collateral circulation following cerebral ischemic stroke. Transl Stroke Res 2018. https://doi.org/10.1007/s12975-018-0638-7.
12. Acar O, Esen T, Colakoglu B, Camli MF, Cakmak YO. Improving testicular blood flow with electroacupuncture-like percutaneous nerve stimulation in an experimental rat model of testicular torsion. Neuromodulation. 2015;18(4):324–8. https://doi.org/10.1111/ner.12246.
13. Hoshikawa R, Kawaguchi H, Takuwa H, Ikoma Y, Tomita Y, Unekawa M, et al. Dynamic flow velocity mapping from fluorescent dye transit times in the brain surface microcirculation of anesthetized rats and mice. Microcirculation. 2016;23(6):416–25. https://doi.org/10.1111/micc.12285.
14. Su T, Wang YB, Wang JD, Han D, Ma S, Cao JB, et al. In vivo magnetic resonance and fluorescence dual-modality imaging of tumor angiogenesis in rats using GEBP11 peptide targeted magnetic nanoparticles. J Biomed Nanotechnol. 2016;12(5):1011–22. https://doi.org/10.1166/jbn.2016.2233.
15. Xu J, Chen A, Xiao J, Jiang Z, Tian Y, Tang Q, et al. Evaluation of tumour vascular distribution and function using immunohistochemistry and BOLD fMRI with carbogen inhalation. Clin Radiol. 2016;71(12):1255–62. https://doi.org/10.1016/j.crad.2016.04.012.
16. Wu XP, Ni JM, Zhang ZY, Lu FQ, Li B, Jin HH, et al. Preoperative evaluation of malignant perihilar biliary obstruction: negative-contrast CT cholangiopancreatography and CT angiography versus MRCP and MR angiography. Am J Roentgenol. 2015;205(4):780–8. https://doi.org/10.2214/Ajr.14.13983.
17. Dehkharghani S, Qiu DQ, Albin LS, Saindane AM. Dose reduction in contrast-enhanced cervical MR angiography: field strength dependency of vascular signal intensity, contrast administration, and arteriographic quality. Am J Roentgenol. 2015;204(6):W701–W6. https://doi.org/10.2214/Ajr.14.13435.
18. Liu P, Sun J, Guan Y, Zhang G, Xu LX. Detection of lung cancer with phase-contrast X-ray imaging using synchrotron radiation. Conf Proc : Annual International Conference of the IEEE Engineering in Medicine and Biology Society IEEE Engineering in Medicine and Biology Society Annual Conference. 2006;1:2001–4. https://doi.org/10.1109/IEMBS.2006.260802.
19. Zhang M, Peng G, Sun D, Xie Y, Xia J, Long H, et al. Synchrotron radiation imaging is a powerful tool to image brain microvasculature. Med Phys. 2014;41(3):031907. https://doi.org/10.1118/1.4865784.
20. Guan Y, Wang Y, Yuan F, Lu H, Ren Y, Xiao T, et al. Effect of suture properties on stability of middle cerebral artery occlusion evaluated by synchrotron radiation angiography. Stroke. 2012;43(3):888–91. https://doi.org/10.1161/STROKEAHA.111.636456.
21. Lu H, Wang Y, He X, Yuan F, Lin X, Xie B, et al. Netrin-1 hyperexpression in mouse brain promotes angiogenesis and long-term neurological recovery after transient focal ischemia. Stroke. 2012;43(3):838–43. https://doi.org/10.1161/STROKEAHA.111.635235.
22. Chen C, Lin X, Wang J, Tang G, Mu Z, Chen X, et al. Effect of HMGB1 on the paracrine action of EPC promotes post-ischemic neovascularization in mice. Stem Cells. 2014;32(10):2679–89. https://doi.org/10.1002/stem.1754.
23. Won SJ, Tang XN, Suh SW, Yenari MA, Swanson RA. Hyperglycemia promotes tissue plasminogen activator-induced hemorrhage by increasing superoxide production. Ann Neurol. 2011;70(4):583–90. https://doi.org/10.1002/ana.22538.
24. Zhang Z, Zhang RL, Jiang Q, Raman SB, Cantwell L, Chopp M. A new rat model of thrombotic focal cerebral ischemia. J Cereb Blood Flow Metab : official journal of the International Society of Cerebral Blood Flow and Metabolism. 1997;17(2):123–35. https://doi.org/10.1097/00004647-199702000-00001.
25. Zhang RL, Chopp M, Zhang ZG, Jiang Q, Ewing JR. A rat model of focal embolic cerebral ischemia. Brain Res. 1997;766(1–2):83–92.
26. Jin R, Zhu X, Li G. Embolic middle cerebral artery occlusion (MCAO) for ischemic stroke with homologous blood clots in rats. J Vis Exp : JoVE. 2014;91:51956. https://doi.org/10.3791/51956.
27. Wang L, Mu Z, Lin X, Geng J, Xiao TQ, Zhang Z, et al. Simultaneous imaging of cerebrovascular structure and function in hypertensive rats using synchrotron radiation angiography. Front Aging Neurosci. 2017;9:359. https://doi.org/10.3389/fnagi.2017.00359.
28. Mu ZH, Jiang Z, Lin XJ, Wang LP, Xi Y, Zhang ZJ, et al. Vessel dilation attenuates endothelial dysfunction following middle cerebral artery occlusion in hyperglycemic rats. CNS Neurosci Ther. 2016;22(4):316–24. https://doi.org/10.1111/cns.12500.
29. Tang Y, Zhang C, Wang J, Lin X, Zhang L, Yang Y, et al. MRI/SPECT/fluorescent tri-modal probe for evaluating the homing and therapeutic efficacy of transplanted mesenchymal stem cells in a rat ischemic stroke model. Adv Funct Mater. 2015;25(7):1024–34. https://doi.org/10.1002/adfm.201402930.
30. Bederson JB, Pitts LH, Germano SM, Nishimura MC, Davis RL, Bartkowski HM. Evaluation of 2,3,5-triphenyltetrazolium chloride

as a stain for detection and quantification of experimental cerebral infarction in rats. Stroke. 1986;17(6):1304–8.
31. Qin C, Zhou P, Wang L, Mamtilahun M, Li W, Zhang Z, et al. Dl-3-N-butylphthalide attenuates ischemic reperfusion injury by improving the function of cerebral artery and circulation. J Cereb Blood Flow Metab : official journal of the International Society of Cerebral Blood Flow and Metabolism. 2018;15:271678X18776833. https://doi.org/10.1177/0271678X18776833.
32. Lin X, Miao P, Wang J, Yuan F, Guan Y, Tang Y, et al. Surgery-related thrombosis critically affects the brain infarct volume in mice following transient middle cerebral artery occlusion. PLoS One. 2013;8(9):e75561. https://doi.org/10.1371/journal.pone.0075561.
33. Kloner RA, King KS, Harrington M. No-reflow phenomenon in heart and brain. Am J Physiol Heart Circ Physiol. 2018;315:H550–62. https://doi.org/10.1152/ajpheart.00183.2018.
34. Dalkara T, Arsava EM. Can restoring incomplete microcirculatory reperfusion improve stroke outcome after thrombolysis? J Cereb Blood Flow Metab : official journal of the International Society of Cerebral Blood Flow and Metabolism. 2012;32(12):2091–9. https://doi.org/10.1038/jcbfm.2012.139.
35. Liu J, Wang Y, Akamatsu Y, Lee CC, Stetler RA, Lawton MT, et al. Vascular remodeling after ischemic stroke: mechanisms and therapeutic potentials. Prog Neurobiol. 2014;115:138–56. https://doi.org/10.1016/j.pneurobio.2013.11.004.
36. Shuaib A, Butcher K, Mohammad AA, Saqqur M, Liebeskind DS. Collateral blood vessels in acute ischaemic stroke: a potential therapeutic target. Lancet Neurol. 2011;10(10):909–21. https://doi.org/10.1016/S1474-4422(11)70195-8.
37. Armitage GA, Todd KG, Shuaib A, Winship IR. Laser speckle contrast imaging of collateral blood flow during acute ischemic stroke. J Cereb Blood Flow Metab : official journal of the International Society of Cerebral Blood Flow and Metabolism. 2010;30(8):1432–6. https://doi.org/10.1038/jcbfm.2010.73.
38. Rosenthal ES, Schwamm LH, Roccatagliata L, Coutts SB, Demchuk AM, Schaefer PW, et al. Role of recanalization in acute stroke outcome: rationale for a CT angiogram-based "benefit of recanalization" model. AJNR Am J Neuroradiol. 2008;29(8):1471–5. https://doi.org/10.3174/ajnr.A1153.
39. Higashida RT, Furlan AJ, Roberts H, Tomsick T, Connors B, Barr J, et al. Trial design and reporting standards for intra-arterial cerebral thrombolysis for acute ischemic stroke. Stroke. 2003;34(8):e109–37. https://doi.org/10.1161/01.STR.0000082721.62796.09.